Journal of Advanced Research in Applied Mechanics 137, Issue 1 (2026) 67-81

SEMARAK ILMU PUBLISHING
202103268166(003316878-P)

Journal of Advanced Research in Applied Mechanics

Journal homepage:
https://semarakilmujournal.com.my/index.php/aram/index
ISSN: 2289-7895

Comparative Analysis of Analytical and Experimental Responses of Cylindrical Metal Structures Subjected to Close-In Blast Loading

Mohd Syedi Imran Mohd Dawi[1,*], Ahmad Humaizi Hilmi[1], Muhamad Saifuldin Abdul Manan[1], Sanusi Hamat[1], Mohd Sabri Hussin[1], Wan Nur A'tiqah Wan Draman[1], Perk Lin Chong[2]

[1] Faculty of Mechanical Engineering and Technology, Universiti Malaysia Perlis, 02600 Arau, Perlis, Malaysia
[2] School of Computing, Engineering & Digital Technologies, Teesside University, Middlesbrough TS1 3BX, United Kingdom

ARTICLE INFO

Article history:
Received 17 March 2025
Received in revised form 20 April 2025
Accepted 27 April 2025
Available online 30 May 2025

Keywords:
Blast loading; single degree of freedom (SDOF) model; close-in blast load

ABSTRACT

The study investigates the deformation behaviour of cylindrical stainless-steel plungers subjected to close-in blast loading, which is important for ensuring structural safety in high-risk environments. While the Single Degree of Freedom (SDOF) model is commonly used for initial evaluations, its accuracy in predicting deformation under such extreme conditions remains uncertain. This research assesses the performance of the SDOF model by comparing its predictions with experimental results from two specimens tested with 100-gram and 250-gram explosive charges. The experimental findings show that segments closest to the blast experience significantly greater deformation than predicted by the SDOF model. The discrepancies result from the SDOF model's inability to fully account for factors like nonlinear material behaviour, strain rate sensitivity and complex boundary conditions, all critical at high strain rates. Although the model assumes a linear reduction in force along the plunger, it could not replicate the rapid energy dissipation observed in the experiments. To address these issues, the study suggests further refinements, including the use of multi-degree of freedom (MDOF) systems, nonlinear material models and finite element analysis (FEA) to better capture dynamic effects and enhance prediction accuracy. These findings highlight the need for more advanced modelling tools to improve the safety and reliability of components designed for blast-prone environments, contributing to safer structural design practices.

1. Introduction

The Single Degree of Freedom (SDOF) system is a tool utilized in structural engineering to evaluate the dynamic behaviour of structures under various loads, including blasts. The SDOF model simplifies structures by representing them as a single mass moving in one direction. This helps engineers analyse the dynamic response without complex calculation. It was useful for blast load scenarios, where rapid force application requires simplified motion equations. The model offers insights into

* *Corresponding author.*
E-mail address: syediimran@unimap.edu.my

https://doi.org/10.37934/aram.137.1.6781

maximum deflection and deformation for the assessment of structural performance and safety under explosive forces [1].

Engineering organizations, such as the American Society of Civil Engineers (ASCE) and the American Institute of Steel Construction (AISC), recommend using the SDOF model to evaluate structural responses under extreme loads. These entities highlight the model's practical efficiency for blast-resistant design. In civil engineering and safety assessments, practitioners frequently use the SDOF method to assess the resilience of structures exposed to potential explosive threats, such as infrastructure or defence systems [2]. Recent studies have demonstrated the relevance of the SDOF model for predicting structural responses under blast loads. For instance, Yan *et al*., [3] extended the SDOF model to include axial loads in steel columns, showing that their predictions match results from both finite element analysis (FEA) and experimental tests. Similarly, Bhatt *et al*., [1] examined the probabilistic behaviour of structural elements subjected to blast loads, validating the model's ability to estimate critical parameters like equivalent stiffness and yield resistance.

The SDOF model provides a rapid assessment tool, enabling engineers to make fast decisions for designing or retrofitting structures to withstand blast events. It also assists in identifying potential failure modes, aiding in the development of strategies to enhance resilience. Given the increasing frequency of explosive incidents globally, the capability to accurately predict structural responses has become essential for public safety and infrastructure reliability [1,3]. Although effective for preliminary analysis, SDOF methods are being integrated with advanced computational models to further refine predictions, resulting in more reliable outcomes for blast-resistant designs [4,5].

There is numerous research focused on blast loads for beams and walls. Various scenarios involving different explosive shapes, weights and distances have been studied. However, the behaviour of cylindrical plungers subjected to close-in blasts remains insufficiently studied. This research examines the deformation of cylindrical metal plungers under blast loading, with the objective of determining whether they can endure repeated use or are compromised after a single application. The analysis addresses a critical gap in the literature by offering a direct comparison between experimental data and SDOF model analytical predictions. This SDOF model of cylindrical plungers also has not been extensively researched within blast engineering. By comparing theoretical predictions with experimental results, the investigation will provide insights into the model performance including strengths and limitations of the model.

There were direct benefits to this research for infrastructure protection, defence and safety-critical systems. Reliable structural design depends on the ability to predict deformation under explosive forces with high accuracy. Resources like AISC Design Guide 26 provide general concepts for blast-resistant structures, despite the current lack of specific requirements for cylindrical plungers. Although the primary focus of this guide is on beams and plates, the SDOF principles may be applied to cylindrical components, offering useful information for dynamic analysis. By means of this validation and analysis, the study provides useful suggestions for safer design and retrofitting techniques, verifying that analytical models agree with practical uses and improve the reliability of structures in harsh environments.

This research illustrates the application of the SDOF model in novel contexts while identifying its limitations. By refining the model and incorporating advanced tools such as FEA, the study provides valuable insights that will enhance future blast-resistant designs. These findings will inform safer engineering practices, ensuring that components exposed to explosive forces are designed with greater precision and reliability.

2. Methodology
2.1 Figure Style and Format

The cylindrical metal plunger response analysis subjected to blast loading can be simplified using a SDOF model. The experiment setup was shown in Figure 1 later translated to the free body diagram shown in Figure 2:

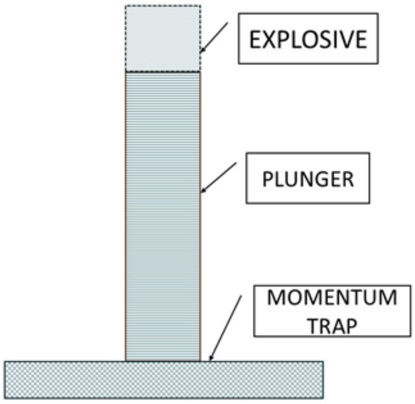

Fig. 1. Experimental setup diagram

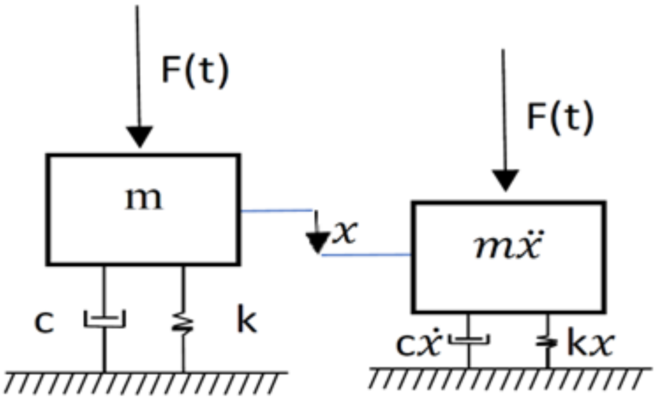

Fig. 2. Free Body Diagram of the idealised system. Equilibrium state (left). After loading (right)

The mass response downward after the force is applied at a certain distance (x). The experiment setup is represented by an equivalent system of mass with gravitational acceleration ($\ddot{x}$), spring representing the resistance to the structure (resisting distance, x) and damper as elastic feature resisting deformation (resisting velocity, $\dot{x}$). According to newton's second law, which is the vector sum of the forces of an object is equal to the mass (assumed mass is constant) multiplied by acceleration ($\sum F = ma$).

The SDOF equation of motion for system under external force $f(t)$ is given as shown in Eq. (1) below:

$$m\ddot{x}(t) + c\dot{x}(t) + kx(t) = f(t) \tag{1}$$

where m is the mass of the plunger segment (kg), c is the damping coefficient (N/m), $x(t)$ is the displacement (deformation) and $f(t)$ is the external force acting on the plunger (blast or applied force). Since the segmented plunger is only mark and the plunger is not cut into segmented, thus, the mass per segment is calculated based on the density of the material. Mass per segment, m_s was compute using Eq. (2):

$$m_s = \rho \cdot V_s = \rho \cdot \left(\frac{\pi d^2}{4} \cdot L_s\right) \tag{2}$$

Where ρ is the density of the material, d is the 50 mm diameter and L_s is the length of each segment which is 20 mm. Stiffness, k the stiffness of each segment can be calculated based on the material's elastic modulus E and its cross-sectional area as shown in Eq. (3):

$$k_s = \frac{E \cdot A}{L_s} = \frac{E \cdot \frac{\pi d^2}{4}}{L_s} \tag{3}$$

Where E is the modulus of elasticity and A is the cross-sectional area of the plunger. The damping coefficient, c will depend on the material's properties and can be taken as $c = 2\zeta\sqrt{k_s m_s}$ where ζ is the damping ratio. SDOF equation is derived for each segment and written as Eq. (4):

$$m_s\ddot{x}(t) + c_s\dot{x}(t) + k_s x(t) = f(t) \tag{4}$$

Where $x(t)$ is the displacement of the segment as a function of time. Harmonic force acting on the plunger (which could represent a blast or other external dynamic force), the external force can be written as:

$$f(t) = F_0 \sin(\omega t) \tag{5}$$

Substitute Eq. (5) into the Eq. (4) equation:

$$m_s\ddot{x}(t) + c_s\dot{x}(t) + k_s x(t) = F_0 \sin(\omega t) \tag{6}$$

Eq. (6) is the second-order linear differential equation and the general solution is of the form:

$$x(t) = x_h(t) + x_p(t) \tag{7}$$

where $x_h(t)$ is the homogeneous solution and $x_p(t)$ is the particular solution. The homogeneous solution solves the equation:

$$m_s\ddot{x}(t) + c_s\dot{x}(t) + k_s x(t) = 0 \tag{8}$$

This leads to the characteristic equation:

$$m_s r^2 + c_s r + k_s = 0 \tag{9}$$

Solving for r:

$$r = \frac{-c_s \pm \sqrt{c_s^2 - 4m_s k_s}}{2m_s} \tag{10}$$

The general solution for the homogeneous part is:

$$x_h(t) = e^{-\zeta\omega_n t}\big(A\cos(\omega_d t) + B\sin(\omega_d t)\big) \tag{11}$$

where $\omega_n = \sqrt{\frac{k_s}{m_s}}$ is the natural frequency, $\omega_d = \sqrt{1-\zeta^2}$ is the damped natural frequency and A and B are constants determined from initial conditions. The particular solution for the force Eq. (5) is given by:

$$x_p(t) = \frac{F_0}{m_s(\omega_n^2 - \omega^2)} \tag{12}$$

Where ω is the driving frequency of the applied force. For each segment of the plunger, the deformation will depend on the cumulative effects from the previous segments, as each segment deforms differently depending on the applied forces and boundary conditions. For Segment A, the displacement based on the above equations using the parameters specific to that segment. For Segment B, the same equations are used but take into account the deformations that occurred in Segment A and so on for the other segments. Thus, the displacement $x_n(t)$ of each segment n would be calculated as:

$$x_n(t) = \frac{F_n}{k_s}\left(1 - e^{-\zeta_n \omega_n t}\left(\cos\left(\omega d_n t\right) + \frac{\zeta_n}{\sqrt{1-\zeta_n^2}}\sin\left(\omega d_n t\right)\right)\right) \tag{13}$$

Where F_n , ω_n and ζ_n correspond to the force, natural frequency and damping ratio for the n-th segment.

2.1.1 Assumptions for the analytical approach

In this analysis, several assumptions were made to simplify the modelling and calculation process while focusing on the primary deformation effects of the plunger subjected to blast loading. First, the plunger material was assumed to be homogeneous and isotropic, implying uniform mechanical properties such as the modulus of elasticity and density across all segments. Stainless Steel 304 was common industrial use and well-known mechanical properties under various loads. The material was modelled with a constant elastic modulus, consistent with previous studies on high strain-rate deformation in metals [6].

The blast force applied to the plunger was assumed to act uniformly across the top surface, resulting in a linear force distribution along the segments. This assumption facilitates segment by segment analysis that simplified the process and aligned with common practices in research involving blast loads on cylindrical metal components [7,8]. By considering the force distribution as uniform, the SDOF model was applied independently to each segment. Potential interactions between adjacent segments or lateral forces were excluded, as similar studies indicated that this approach successfully simplifies the analysis of dynamic systems subjected to blast loads [6,9].

The model used also did not account for damping effects and time-dependent forces but focusing solely on static deformation caused by the explosive load. This method is consistent with early-stage analytical models, where static analysis establishes a baseline for structural response prior to incorporating dynamic complexities [8]. The boundary conditions were also simplified by fully constraining the base of the plunger, where any displacement or rotation is not included. Such boundary conditions are frequently used in blast simulations to streamline the calculation of deformation while accurately capturing essential structural behaviour [7].

Abaqus simulation software was utilized to estimate the pressure exerted on the top end surface (closest to the point of detonation). This method is widely used in blast-related studies to predict pressures from close-in explosions, particularly when obtaining experimental data is challenging or impractical [6]. Numerical simulations like these offer reliable estimates of blast-induced pressure, enabling accurate predictions in scenarios where physical testing is limited or constrained by safety concerns.

2.1.2 Damping ratio assumption

304 stainless steel was dynamically simulated under high-strain-rate conditions caused by blast loading using a damping ratio of 0.005 (5%). Other research that investigated at how the material behaved during plastic deformation and energy dissipation supports this value [4,7]. Although metals typically exhibit low damping ratios (0.01 to 0.02) within their elastic range, these values notably increase with higher strain rates and plastic deformation [7,8]. Research conducted by Colakoglu *et al.,* [9] demonstrated rising damping values in cyclic fatigue tests as deformation approached fatigue crack initiation. Further studies on blast and dynamic loading also support the application of a 5% damping ratio for enhanced energy dissipation during rapid deformation [6,8]. This ratio is suitable for engineering applications that need computing efficiency because it successfully balanced between capturing the materials dynamic response and maintaining modelling simplicity [7].

2.1.3 Pressure value

Due to the complexity of experimental for blast testing, the force (*F*) value was determined through simulation as direct measurement poses safety challenges. Simulations offer greater control over test conditions, permitting the examination of various parameters and their impacts on the deformation behaviour of the solid cylindrical plunger.

Recent research points out the ability of numerical simulations in predicting structural behaviour under blast loads, particularly for components subjected to axial forces [10,11]. For example, Al-Thairy [12] developed a finite element model using ABAQUS/Explicit to simulate steel column responses under explosive loads, with validation against experimental data. This validation confirms that simulations can capture the dynamic behaviour of materials during blast events accurately. Similarly to Shuaib *et al*., [13] highlighted the increasing reliance on finite element methods (FEM) for evaluating material responses to blast loads, further supporting the reliability of numerical approaches in producing results comparable to physical tests. The study by Wei *et al*., [14] also validates the use of simulations, particularly for cylindrical structures. Their investigation into the impact of blast loads on cylindrical shells combined experimental tests with simulations, providing valuable insights into pressure distribution and the resulting forces experienced by structures during explosions.

Thus, the decision to derive force values through simulation was indeed acceptable. This approach not only mitigates the risks associated with live blast testing but also provides a comprehensive understanding of how various parameters influence structural deformation. It also enables more informed engineering decisions and ensures that critical factors affecting deformation are thoroughly evaluated.

Figure 3 (left) illustrates the FEM model, comprising the explosive, specimen and base plate, all meshed using eight-node linear brick elements (C3D8R). Each component is positioned directly on top of the other with no gaps between them. As shown in Figure 2, the bottom surface of the momentum trap is fixed to replicate the actual boundary conditions. To maintain this positioning, encastre boundary conditions (U1 = U2 = U3 = UR1 = UR2 = UR3 = 0) were applied to the base plate's bottom surface, restricting all translations and rotations. Also, a general contact interaction was assigned across all model components to simulate realistic contact behaviour. Based on the Pressure vs. Time graph generated through the Abaqus simulation (as shown in Figure 3 (right)), which analysed approximately 300 nodes on the top surface of the plunger, the pressure values were assessed to determine the most appropriate input for the Single Degree of Freedom (SDOF) calculation. The graph displays an initial peak pressure of around 2250 N/mm² in the +Y direction, representing the upward force immediately following the explosion. However, since the SDOF calculation focuses on the deformation in the -Y direction (downward), the force responsible for the downward deformation must be accurately represented. Using the maximum pressure in the +Y direction could lead to an overestimation of the force acting in the -Y direction, as the upward pressure reflects the reactive force rather than the primary impact force driving the deformation.

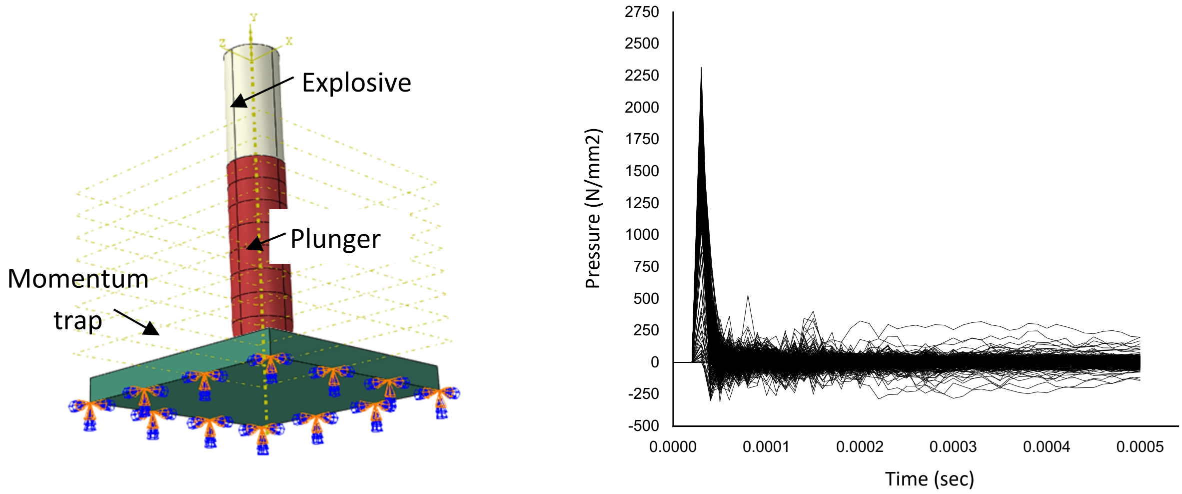

Fig. 3. Simulation model (left); Example of Pressure vs. Time graph for 250-gram explosive (right)

For accurate SDOF modelling, it is essential to select the pressure corresponding to the -Y direction (downward), which directly reflects the explosive force that causes the deformation. Previous research has emphasized the importance of considering the correct force direction when modelling deformation under blast loads, as the force components acting against the primary direction of interest (such as in the +Y direction) can distort the results if incorrectly factored into calculations [7]. This pressure represents the true impact force exerted on the plunger surface in the direction of interest. Therefore, while the graph indicates a maximum pressure of more than 2000 N/mm² in the +Y direction, the value used for SDOF calculations should be based on the peak pressure in the -Y direction, which is more relevant for evaluating the structural response to the blast. This approach ensures that the model captures the correct force acting on the plunger, leading to accurate and realistic predictions of deformation in response to the blast. Thus, the value chosen was 309.19 N/mm^2 (for 250-gram explosives weight) where converted into force,F for calculation become 626676 N. Table 1 listed the material properties of stainless steel 304 use for calculation.

Table 1
Material property for stainless steel 304 [8]

Properties	
Elastic Modulus, E	200 GPa / 200×10^9 N/m^2
Density, ρ	7900 kg/m^3
Poisson's ratio	0.3
Damping ratio	0.05

The approximate initial geometry of both specimen A and B listed in Table 2.

Table 2
Specimen geometry

Properties	Dimension(mm)
Diameter	50.8
Length	180

2.1.4 Linear attenuation approach

In a close-in blast scenario, where the blast point occurs on the top surface of the plunger (Segment A), the force would not be uniform across all segments. Instead, the force is expected to decay as it travels down the plunger due to the dissipation of energy. This decay can be modelled using an exponential or linear attenuation of the blast force. The force will be highest at Segment A (closest to the blast) and gradually decrease through the lower segments (B to I). A common approach to model this decays in force is to assume that the force follows an exponential decay or linear attenuation based on distance from the blast point. However, this study will use linear attenuation approach by using the following equation:

$$F_n = F_A.\left(1 - \frac{n-1}{N-1}\right) \tag{14}$$

Where F_n is the force on segment n , F_A is the initial force at Segment A and N is the total number of segments 9 in this study)

2.2 Experimental Setup

The experiment utilized cylindrical solid metal specimens made from 304 stainless steel, referred to as "plungers," subjected to close-in blast loading. The explosive material was placed directly on the top surface of the plunger, as depicted in Figure 4. Two specimens (specimen A and B) were prepared for comparison, subjected to explosive charges of 100 grams and 250 grams, respectively.

Fig. 4. Experimental setup for specimen B with 250-gram explosive on top

Prior to the experiment, each plunger was prepared by marking nine segments, each 20 mm in length, using a Mitutoyo Vernier Height Gauge. These segments were marked from the top end of the plunger (closest to the detonation point) and labelled sequentially as A (top) through I (bottom), as shown in Figure 5 and Figure 6. The consistent segment length of 20 mm was deemed sufficient for capturing dimensional changes across the plunger, from the point closest to the detonation (Segment A) to the furthest point (Segment I).

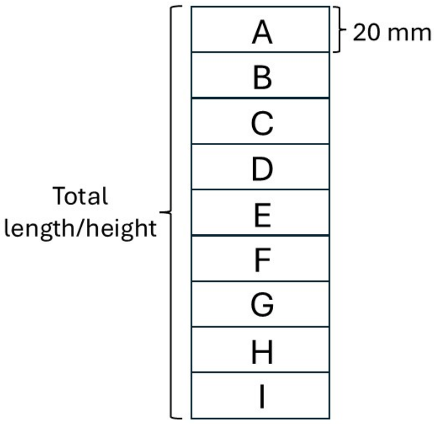

Fig. 5. Diagram of the segmented plunger

Fig. 6. Marking process using the Vernier Height Gauge

The plungers were subjected to close-in blast loading by placing the explosive material directly on the top surface. The detonation caused rapid deformation across the segments, with the expectation that segments closer to the detonation point (Segment A) would experience the highest deformation, while the segments furthest away (Segment I) would experience minimal deformation. Two sets of experiments were conducted, one with a 100-gram explosive charge and the other with a 250-gram charge. Post-detonation, the deformed dimensions of each segment were measured using a Mitutoyo Digital Vernier Calliper to quantify the changes in length and diameter of the plunger segments. The value is recorded for further analysis.

2.3 Validation and Comparison

The experimental results were compared with predictions from an analytical model designed to estimate dimensional changes in the segments of the plunger after blast exposure. This analytical model is based on the Second-Order Single Degree of Freedom (SDOF) system, which calculates the expected deformation of each segment along the Y-axis (lengthwise). The Y-axis deformation was chosen as the focus since it aligns with the direction of the blast force, making it the most critical dimension for assessing the impact of the explosive load on the structure.

Measurements of each segment's deformation following detonation were made and the results were compared to the predictions of the analytical model. Using a Mitutoyo Digital Vernier Calliper, post-blast segment lengths were precisely measured, ensuring data gathering accuracy. The model's ability to predict deformation was evaluated by directly comparing the analytical results with the experimental observations.

Two specimens were examined using 100 gram and 250 grams of explosive charges, respectively, to further verify the comparison. This made it possible to assess the model's capacity for predicting deformation over a range of blast intensities in greater detail. In order to determine possible sources of error, differences between the analytical and experimental data were closely examined. Variations in material qualities, the boundary conditions used or assumptions made within the analytical model could have all contributed to these disparities. This validation process provides a critical assessment of the analytical model's accuracy, highlighting both the predictive strengths and areas where further refinement may be needed.

3. Results and Discussion

3.1 Experimental and Analytical Result

The experimental and calculated results for Specimen A and Specimen B reveal significant differences in deformation across the segments, reflecting both the limitations of the analytical model and the complex behaviour of the material under blast loading. Specimen A shows the largest deformation (see Table 3) at Segment A (1.31 mm), which is closest to the blast, with minimal deformation in segments further away (Segments C to G). There is a small amount of residual deformation in Segment H (0.05 mm) and Segment I (0.02 mm).

Table 3
Specimen A experimental result

Segment	Initial length (mm)	Final length (mm)	Deformation (mm)
A	20.00	18.69	1.31
B	20.00	19.08	0.92
C	20.00	20.00	-
D	20.00	20.00	-
E	20.00	20.00	-
F	20.00	20.00	-
G	20.00	20.00	-
H	20.00	19.95	0.05
I	20.00	19.92	0.02

Specimen B (see Table 4) also exhibits the highest deformation in Segment A (1.65 mm). However, unlike Specimen A, Specimen B shows more notable deformations in Segment C (0.12 mm) and Segment G (0.13 mm). This suggests slight variations in how the blast energy was dissipated across the specimens.

Table 4
Specimen B experimental result

Segment	Initial length (mm)	Final length (mm)	Deformation (mm)
A	20.00	18.35	1.65
B	20.00	19.80	0.2
C	20.00	19.88	0.12
D	20.00	20.00	-
E	20.00	20.00	-
F	20.00	20.00	-
G	20.00	19.87	0.13
H	20.00	20.00	-
I	20.00	19.77	0.23

However, the analytical model predicts much smaller deformations for both specimens across all segments (see Table 5). For example, Segment A in Specimen A is predicted to deform by only 0.03 mm, which is significantly lower than the 1.31 mm observed experimentally. Similar underestimations are seen in Specimen B, where the calculated deformation for Segment A is 0.0309 mm compared to the 1.65 mm recorded in the experiment.

Table 5
Deformation calculated result

Segments	Specimen A *Deformation (mm)*	Specimen B *Deformation (mm)*
A	0.0300	0.0309
B	0.0266	0.0275
C	0.0232	0.0239
D	0.0199	0.0205
E	0.0166	0.0170
F	0.0132	0.0135
G	0.0987	0.0101
H	0.0651	0.0066
I	0.0036	0.0036

The experimental and analytical results is further evaluated to measure the discrepancy as shown in Table 6 below. The discrepancies are high for most segments, especially in Segment A, where the difference between experimental and analytical results exceeds 97% for both specimens. Some segments with zero experimental deformation (e.g., C, D, E) show discrepancies as N/A, indicating no experimental deformation occurred. Specimen B shows slightly higher deformations than Specimen A in certain segments, but both specimens reveal significant differences compared to the analytical predictions.

Table 6
Deformation calculated result

Segment	Exp A (mm)	Ana A (mm)	Discrepancy A (%)	Exp B (mm)	Ana B (mm)	Discrepancy B (%)
A	1.31	0.0300	97.71	1.65	0.0309	98.13
B	0.92	0.0266	97.11	0.20	0.0275	86.25
C	0.00	0.0232	N/A	0.12	0.0239	80.08
D	0.00	0.0199	N/A	0.00	0.0205	N/A
E	0.00	0.0166	N/A	0.00	0.0170	N/A
F	0.00	0.0132	N/A	0.00	0.0135	N/A
G	0.00	0.0987	N/A	0.13	0.0101	92.23
H	0.05	0.0651	30.20	0.00	0.0066	N/A
I	0.02	0.0036	82.00	0.23	0.0036	98.43

The experimental and analytical results for Specimen A and Specimen B reveal important insights into the behaviour of the cylindrical stainless-steel plungers under blast loading. Table 7 shows that the calculated values are the same across all segments.

Table 7
Calculated value for 304 stainless steels

Mass, m_s (kg)	Stiffness, k_s (N/m)	Damping coefficient, c (kg/s)	Natural Frequency, ω_n (rad/s)	Damped Frequency, ω_d (rad/s)
0.3202	20268299163.899	8056.4896	251577.3027	251262.6342

Using a simulation to estimate the blast force, the linear attenuation of force was calculated and the results for both specimens are shown in Table 8 which later use to calculate the deformation value.

Table 8
Calculated force of decay value

Segments	Specimen A *Force (N)*	Specimen B *Force (N)*
A (simulation)	608049	626676
B	540044	556390
C	472039	486105
D	404033	415820
E	336028	345535
F	268023	275250
G	200018	204965
H	132012	134680
I	64007	64395

The use of a linear attenuation of force in the analytical model produced force values that steadily decreased from Segment A to Segment I. While this approach captures the trend of decreasing deformation with distance from the blast, the model still underestimates the force absorption capacity of the material at the segment level. The experimental data shows that deformation sharply decreases after Segment A, particularly in Specimen A, where most segments experience no deformation. However, the analytical model predicts a more gradual reduction in deformation across the segments. This suggests that the linear attenuation of force used in the model does not accurately represent how the blast energy dissipates, particularly in terms of the sharp energy drop-off observed experimentally.

3.2 Limitations of the SDOF Model

The analytical model used in this research using a linear elastic response for Stainless Steel 304, which does not accurately reflect the behaviour under high-energy impacts subjected by blast loads. Experimental findings indicate that Stainless Steel 304 undergoes significant plastic deformation in such extreme conditions. It was an important factor not captured by the SDOF model [15]. As the material transitions from elastic to plastic states, the nonlinear stress-strain behaviour results in increased deformation. This highlights the importance of integrating material nonlinearity into analytical models to enhance predictive accuracy.

The SDOF model also does not account for the high strain rates characteristic of blast scenarios. The mechanical properties of stainless steel, such as yield strength and ductility, change considerably under these conditions, contributing to the discrepancies between experimental outcomes and analytical predictions [16]. Research demonstrates that as strain rates increase, the yield strength of Stainless Steel 304 also rises, altering its deformation characteristics. These variations are not represented in the SDOF model, which adds to the limitations of the current analytical approach.

The SDOF model assumes uniform deformation, simplifying boundary conditions. However, the plunger's actual behaviour involves complex base and length interactions with multiple deformation modes. This often leads to the model underestimating deformation, especially in areas far from the blast source [17]. Advanced modelling approaches are necessary to address boundary interactions and nonlinear material properties. Studies by Sauer *et al.*, [7] and Wang *et al.*, [18] show that Finite Element Analysis (FEA) effectively captures deformations and failure mechanisms under extreme conditions. The SDOF model's limitations in handling nonlinear material responses, strain rate effects and complex boundary conditions highlight the need for advanced simulation methods to accurately represent Stainless Steel 304 under blast loading.

3.3 Refinements and Sophisticated Modelling Techniques

Multi-Degree of Freedom (MDOF) systems in modelling provides more realistic way to represent dynamic behaviour where each segment of the plunger can be modelled as an independent mass and each with unique stiffness and deformation properties. This setup allows for the consideration of higher-order dynamic effects, such as vibrations and localized deformations that occur at different points along the plunger when subjected to explosive forces. Accurately capturing these interactions is essential for reliable predictions of the structural response under extreme loading conditions [13].

Improving the predictions model involves incorporating material nonlinearity and strain rate effects. The Johnson-Cook model effectively simulates material behaviour under high strain rates and plastic deformation, making it useful for analysing materials like Stainless Steel 304 exposed to blast loads. This model has shown reliable results in studies on metal impact and blast behaviour, often aligning with experimental observations [19,20].

Finite Element Modelling (FEM) effectively addresses complex interactions among material properties, boundary conditions and strain rate effects. FEM simulations can account for material nonlinearity and intricate boundary conditions, leading to accurate predictions of deformation under blast conditions. Studies validate FEM's effectiveness in simulating deformations and identifying failure mechanisms in structures under extreme forces [21,22]. These detailed insights are important for understanding how materials and structures react to blast loads, helping to improve design and safety measures, as shown by Kasim *et al*., [23]. Simulation techniques are essential for testing safety designs and predicting pressure distribution in extreme conditions.

4. Conclusions

The research studies the accuracy of SDOF model in predicting stainless steel deformation subjected to close-in blast loads. Base on the experiments with 100-gram and 250 grams explosive charges shows significant discrepancies occurs due to the SDOF model underestimating deformation near the point of detonation. This shows the model limitations in considering for high-strain-rate dynamics, strain rate sensitivity, material nonlinearity and boundary conditions.

The simplified assumption of linear force attenuation used in the SDOF model did not accurately represent the energy decline observed in the experimental data, resulting in differences between observed and predicted deformations. This indicates that, while the SDOF model is useful for initial assessments, it may not be suitable for high-energy, dynamic environments where precise deformation predictions are necessary. Advanced modelling techniques such as multi-degree of freedom (MDOF) systems and finite element analysis (FEA), should be considered. These methods can better account for material behaviour under high strain rates and include nonlinear deformation effects. Constitutive models like the Johnson-Cook model could also enhance predictive accuracy, as they are designed to simulate the dynamic responses of materials, including plastic deformation and strain rate sensitivity.

It also recommended that for future experiments to use multiple specimens for each explosive charge to improve data reliability. This study was limited to testing only one plunger per charge due to controlled environment restrictions and safety considerations. Increasing the number of repetitions would give robust statistical data and further validate the findings. This work highlights the need for advanced modelling to align theory with experiments, enhancing our understanding of structural behaviour under extreme conditions and leading to safer, more resilient structures against explosive forces.

Acknowledgement
This research was funded by a grant from Ministry of Higher Education of Malaysia (FRGS Grant FRGS/1/2018/TK03/UNIMAP/02/21).

References
[1] Bhatt, Anita, Priti Maheshwari and Pradeep Bhargava. "Probabilistic performance analysis of structural elements subjected to blast load using equivalent static force model." *International Journal of Protective Structures* 15, no. 1 (2024): 65-94. https://doi.org/10.1177/20414196221142905
[2] Singh, Karandeep, Paolo Gardoni and Flavio Stochino. "Probabilistic models for blast parameters and fragility estimates of steel columns subject to blast loads." *Engineering Structures* 222 (2020): 110944. https://doi.org/10.1016/j.engstruct.2020.110944
[3] Yan, Junbo, Yan Liu and Fenglei Huang. "Improved SDOF approach to incorporate the effects of axial loads on the dynamic responses of steel columns subjected to blast loads." *Advances in Civil Engineering* 2019, no. 1 (2019): 7810542. https://doi.org/10.1155/2019/7810542
[4] Pezzola, G. L., L. K. Stewart and G. Hegemier. "Analysis methods for CFRP blast retrofitted reinforced concrete wall systems." *International Journal of Computational Methods and Experimental Measurements* 4, no. 3 (2016): 247-257. https://doi.org/10.2495/CMEM-V4-N3-247-257
[5] Rigby, Sam E. andrew Tyas, Sam D. Clarke and Ghani Razaqpur. "Approach to developing design charts for quantifying the influence of blast wave clearing on target deformation." *Journal of Structural Engineering* 143, no. 1 (2017): 04016150. https://doi.org/10.1061/(ASCE)ST.1943-541X.0001626
[6] De Finis, Rosa, Davide Palumbo and Umberto Galietti. "Mechanical behaviour of stainless steels under dynamic loading: An investigation with thermal methods." *Journal of Imaging* 2, no. 4 (2016): 32. https://doi.org/10.3390/jimaging2040032
[7] Sauer, C. andreas Heine and Werner Riedel. "Comprehensive study of projectile impact on lightweight adobe masonry." *International Journal of Impact Engineering* 125 (2019): 56-62. https://doi.org/10.1016/j.ijimpeng.2018.10.010
[8] Remennikov, Alex and David Carolan. "Blast effects and vulnerability of building structures from terrorist attack." *Australian Journal of Structural Engineering* 7, no. 1 (2006): 1-11. https://doi.org/10.1080/13287982.2006.11464959
[9] Colakoglu, M. and K. L. Jerina. "Damping behaviour of cyclically deformed 304 stainless steel." (2003).
[10] Ismail, M. S., BTH T. Baharudin, S. A. Yahya and H. A. Kahar. "Finite element analysis of composite cylinder with centre cutout under axial load and internal pressure." *Advanced Materials Research* 701 (2013): 425-429. https://doi.org/10.4028/www.scientific.net/AMR.701.425
[11] Ismail, Mohd Shahrom, Farhah Nadhirah Nordin, Chi Hieu Le, Ho Quang Nguyen and Jamaluddin Mahmud. "The implementation of the single perturbation load approach to axially-compressed stiffened-stringer cylinder." In *Innovative Manufacturing, Mechatronics & Materials Forum*, pp. 13-23. Singapore: Springer Nature Singapore, 2023. https://doi.org/10.1007/978-981-99-9848-7_2
[12] Al-Thairy, Haitham. "Behaviour and failure of steel columns subjected to blast loads: Numerical study and analytical approach." *Advances in Materials Science and Engineering* 2018, no. 1 (2018): 1591384. https://doi.org/10.1155/2018/1591384
[13] Shuaib, Mujtaba M., Steeve Chung Kim Yuen and Gerald N. Nurick. "Numerical simulation of blast loaded CFRP retrofitted steel plates." In *MATEC Web of Conferences*, vol. 347, p. 00038. EDP Sciences, 2021. https://doi.org/10.1051/matecconf/202134700038
[14] Wei, Wuchen, Dianshuang Zheng, Di Yang, Hongchi Guo, Fei Yin and Xudong Zhi. "Experimental and simulation study on blast loads of cylindrical Shells." *Advances in Structural Engineering* 26, no. 4 (2023): 679-692. https://doi.org/10.1177/13694332221135896
[15] Walport, Fiona, Leroy Gardner, Esther Real, Itsaso Arrayago and David A. Nethercot. "Effects of material nonlinearity on the global analysis and stability of stainless steel frames." *Journal of Constructional Steel Research* 152 (2019): 173-182. https://doi.org/10.1016/j.jcsr.2018.04.019
[16] Barbosa, Patrícia Alves and Izabel Fernanda Machado. "Strain rate effect on the mechanical behavior of austenitic stainless steel during machining." *Advanced Materials Research* 223 (2011): 332-339. https://doi.org/10.4028/www.scientific.net/AMR.223.332
[17] Fekry, Asmaa A., Amr A. Nassr, Ahmed M. Ismail, Eslam M. Soliman and Ali Gamal. "Behavior Of Steel Hollow Sections Under Blast Load." *Journal of Advanced Engineering Trends* 39, no. 2 (2020): 121-134. https://doi.org/10.21608/jaet.2020.96450

[18] Wang, Zhanjun, Desislava Karagiozova, Shanjun Li and Bo Yu. "Numerical Investigation of Failure Mechanisms in Stainless Steel Tubes Subjected to Close-in Explosions." *International Journal of Protective Structures 11(3), (*2020): 285–306. https://doi.org/10.1177/2041419620938991
[19] Imran, Mohd Syedi, Ahmad Humaizi Hilmi, Muhamad Saifuldin Abdul Manan, Ahmad Mujahid Ahmad Zaidi, Mohd Sabri Hussin and Perk Lin Chong. "Numerical and Experimental Investigation on Aluminium 6061 Solid Cylindrical Bar Subjected to Close-in Blast Loading." *Journal of Advanced Research in Applied Mechanics* 113, no. 1 (2024): 138-151. https://doi.org/10.37934/aram.113.1.138151
[20] Fu, Feng. "Assessment of the progressive collapse potential in tall buildings with 3D FE method." In *Structures Congress 2014*, pp. 847-856. 2014. https://doi.org/10.1061/9780784413357.075
[21] Phadnis, Vaibhav A., Puneet Kumar, Arun Shukla, Anish Roy and Vadim V. Silberschmidt. "Optimising curvature of carbon fibre-reinforced polymer composite panel for improved blast resistance: finite-element analysis." *Materials & Design* 57 (2014): 719-727. https://doi.org/10.1016/j.matdes.2014.01.034
[22] Gharehdash, Saba, Lu Ming Shen, Yi Xiang Gan and E. A. Flores-Johnson. "Numerical investigation on fracturing of rock under blast using coupled finite element method and smoothed particle hydrodynamics." *Applied Mechanics and Materials* 846 (2016): 102-107. https://doi.org/10.4028/www.scientific.net/AMM.846.102
[23] Kasim, Mohd Shahir, Siti Nurul Akmal Yusof, Ruwaidi Mat Rasul, Roslan Awang, Zammeri Abd, Saiful Bahri Mohamed Rahman, Taufik Roni Sahroni and Md Anayet Ullah Patwari. "Design and Optimization of LPG Safety Cap using Finite Element Method." *safety* 54, no. 2 (2025): 191-199. https://doi.org/10.37934/araset.54.2.191199